

# Quantum Phase Transitions of Frustrated Heisenberg Antiferromagnets: a Comprehensive Renormalization Approach

Frank Krüger and Stefan Scheidl

*Institut für Theoretische Physik, Universität zu Köln, Zùlpicher Str. 77, D-50937 Köln, Germany*

(Dated: November 21, 2018)

We develop a novel renormalization approach for frustrated quantum antiferromagnets. It is designed to consistently treat spin-wave interactions all over the magnetic Brillouin zone, including high-energy modes in outer regions as well as low energy modes in the center. Focusing on the paradigmatic  $J_1$ - $J_2$  model, we find a unifying description of the second-order transition between the Néel phase and the paramagnetic phase and the first-order transition between the Néel phase and the columnar phase. Our approach provides explicit results for the renormalized values of the spin stiffness and spin-wave velocity characterizing the low-energy magnons in the Néel phase.

PACS numbers: 75.30.Kz, 75.50.Ee, 75.10.Jm, 05.10.Cc

Frustrated magnets exhibit quantum phase transitions of a rich variety which is subject of intensive current research [1]. Novel scenarios for phase transitions beyond the Landau-Ginzburg-Wilson paradigm have been suggested [2] and juggle fundamental concepts. The Heisenberg model on a square lattice with antiferromagnetic couplings  $J_1$  and  $J_2$  between nearest and next-nearest neighbors serves as a prototype for studying magnetic quantum-phase transitions (see, e.g., [3] and references therein). From the classical limit one expects that two different magnetic orders can exist: the Néel phase with ordering wave vector  $(\pi, \pi)$  is favorable for  $\alpha \equiv J_2/J_1 < 1/2$  and columnar order with  $(0, \pi)$  for  $\alpha > 1/2$ .

Quantum fluctuations certainly may induce a paramagnetic (PM) phase which is naturally expected near  $\alpha \approx 1/2$  where both orders compete [4]. Remarkably, additional orders may appear in the Néel phase as well as in the PM phase when translation symmetry is broken by an additional spin dimerization. The existence of such enhanced order crucially depends on the spin value  $S$ . This becomes most apparent when the spin system is represented by a nonlinear-sigma model. Topological excitations can give rise to a four-fold ground-state degeneracy if  $S + 1/2$  is integer, and a twofold degeneracy if  $S$  is odd [5, 6]. These degeneracies correspond to a translation-symmetry breaking by dimerization.

Field-theoretical approaches have been started from various sides, based on the  $1/S$  [7] or the  $1/N$  expansion [8, 9]. The latter approach is able to capture some essence of the topological aspects on a mean-field level. However, it is the former approach, elaborated to a renormalization-group analysis, which predominantly has served as basis for a comparison of critical aspects between theory and experiment (see e.g. [10]).

Nevertheless, this approach so far has suffered from two intrinsic shortcomings: i) Spin-wave interactions are the physical mechanism underlying the renormalization flow. On one-loop level, the flow equations describe corrections to the physical parameters of relative order  $1/S$ . These corrections have been worked out using a continuum ver-

sion of the nonlinear  $\sigma$  model (CNL $\sigma$ M) as a starting point [7]. However, for the original lattice model, this is not systematic, since corrections of the same order are dropped under the mapping of the lattice model onto the CNL $\sigma$ M. As a consequence, important effects such as a renormalization of the spin-wave velocity are missed. ii) Simultaneously, the outer region of the magnetic Brillouin zone (BZ) is only crudely treated. This entails a quantitatively significant uncertainty for the prediction of the location of the phase boundary.

In this Letter, we lift these shortcomings by developing a renormalization analysis which fully accounts for the lattice structure. It combines the systematic treatment of all corrections in order  $1/S$  on the level of the conventional first-order spin-wave theory (SWT) with the merits of a renormalization approach, which goes beyond any finite order in  $1/S$  by an infinite iteration of differential steps, which successively eliminate the spin-wave modes of highest energy. As a result, we obtain an improved description of the phase transitions. Its only remaining drawback is the neglect of topological excitations. From a comparison of our results with experimental data one may therefore gain deeper insight into the quantitative relevance of these excitations.

To be specific, we stick to the aforementioned  $J_1$ - $J_2$  Heisenberg model on a square lattice. We address the stability of the Néel phase against quantum fluctuations controlled by  $S$  and  $\alpha$ . Fluctuations are treated in a coherent spin state path-integral representation of the model, where a spin state corresponds to a unit vector  $\vec{n}$ . In the absence of fluctuations, spins would assume the states  $|\vec{n}_{A/B}\rangle = |\pm \vec{e}_z\rangle = |S, \pm S\rangle$  on the two sublattice A and B. From the standard Trotter formula emerges an imaginary time  $\tau$  (discretized in intervals of duration  $\Delta\tau$ ) and an action of the form [1]

$$\mathcal{S} = - \sum_{\tau} \ln \langle \{\vec{n}\} | \{\vec{n}'\} \rangle + \sum_{\tau} \Delta\tau \frac{\langle \{\vec{n}\} | \hat{H} | \{\vec{n}'\} \rangle}{\langle \{\vec{n}\} | \{\vec{n}'\} \rangle} \quad (1)$$

taking  $\vec{n}$  at time  $\tau$  and  $\vec{n}'$  at  $\tau - \Delta\tau$ . For weak quantum fluctuations, the components of  $n_{x,y}$  perpendicular to

the magnetization axis are small and may be considered as expansion parameters (as in [7]). However, attempting to directly apply this expansion to the lattice model we encountered time ordering difficulties in the action [11].

Instead, we start from a stereographic parametrization of coherent states, on sublattice A.  $|\vec{n}\rangle = (1 + \bar{a}a/2S)^{-S} \exp(a\hat{S}_-/\sqrt{2S})|S, S\rangle$  where  $a$  is the stereographic projection of  $\vec{n}$  from the unit sphere onto the complex plane,  $a = \tan(\theta/2) \exp(i\phi)$  with the standard spherical angles  $\theta$  and  $\phi$ . The action can be expressed in terms of the stereographic coordinates using the matrix elements[12]

$$\frac{\langle \vec{n} | \hat{S}_z | \vec{n}' \rangle}{\langle \vec{n} | \vec{n}' \rangle} = S \frac{1 - \bar{a}a'/2S}{1 + \bar{a}a'/2S}, \quad \frac{\langle \vec{n} | \hat{S}_+ | \vec{n}' \rangle}{\langle \vec{n} | \vec{n}' \rangle} = \frac{\sqrt{2S} a'}{1 + \bar{a}a'/2S}$$

( $\bar{a}$  is the complex conjugate of  $a$ ) and analogous expressions for the coordinate  $b$  on sublattice B [13].

The explicit expression of the action in terms of  $a$  and  $b$  is too lengthy to be given here. To leading order in  $1/S$ , the fluctuations are controlled by the bilinear part  $\mathcal{S}_0$  of the action that represents free magnons. We also retain the quartic contribution  $\mathcal{S}_{\text{int}}$  to the action, which represents magnon interactions and contain the renormalization of single-magnon parameters of relative order  $1/S$ . Higher order contributions to the action are neglected. Terms from the functional Jacobian are also negligible on this level. The single-magnon contribution to the action can be parameterized in the form

$$\mathcal{S}_0 = \sum_{\tau} \int_{\mathbf{k}} \left\{ \frac{1}{2g} [\bar{a}_{\mathbf{k}} \Delta a_{\mathbf{k}} - \Delta \bar{a}_{\mathbf{k}} a'_{\mathbf{k}} + \bar{b}_{\mathbf{k}} \Delta b_{\mathbf{k}} - \Delta \bar{b}_{\mathbf{k}} b'_{\mathbf{k}}] + \Delta \tau S [\Gamma_{\mathbf{k}}^+ (\bar{a}_{\mathbf{k}} a'_{\mathbf{k}} + \bar{b}_{\mathbf{k}} b'_{\mathbf{k}}) + \Gamma_{\mathbf{k}}^- (\bar{a}_{\mathbf{k}} \bar{b}_{\mathbf{k}} + a'_{\mathbf{k}} b'_{\mathbf{k}})] \right\}, (2)$$

using the Fourier transform  $a(\mathbf{r}) = \int_{\mathbf{k}} e^{i\mathbf{k}\cdot\mathbf{r}} a_{\mathbf{k}}$ , the integral  $\int_{\mathbf{k}} = 2 \int \frac{d^2k}{(2\pi)^2}$  over the magnetic BZ  $|k_x| + |k_y| \leq \pi$ , and the exchange couplings  $\Gamma_{\mathbf{k}}^+ \equiv J_{\mathbf{k}}^+ - J_0^+ + J_0^-$ ,  $\Gamma_{\mathbf{k}}^- \equiv J_{\mathbf{k}}^- \equiv 2J_1[\cos(k_x) + \cos(k_y)]$  and  $J_{\mathbf{k}}^+ = 2J_2[\cos(k_x + k_y) + \cos(k_x - k_y)]$ . For simplicity the lattice constant is considered as unit length. The dimensionless parameter  $g$  represents the strength of quantum fluctuations. It assumes the value  $g = 1$  in the unrenormalized model and turns out to increase under renormalization.

Diagonalizing this bilinear action, one easily obtains the magnon energies  $E_{\mathbf{k}} = Sg|\Gamma_{\mathbf{k}}^+| \sqrt{1 - \gamma_{\mathbf{k}}^2}$ , where  $\gamma_{\mathbf{k}} = \Gamma_{\mathbf{k}}^-/\Gamma_{\mathbf{k}}^+$ . For  $\alpha \leq 1/2$ , the low-energy spin-wave excitations are characterized by an isotropic dispersion  $E(\mathbf{k}) = c|\mathbf{k}| + O(k^2)$  with a spin-wave velocity  $c = \sqrt{8gSJ_1\sqrt{1-2\alpha}}$ . Likewise, the exchange couplings generate a spin stiffness  $\rho = S^2J_1(1-2\alpha)$  for low-energy modes. One also obtains the propagators  $\langle \bar{\phi}_{\mathbf{k}} \phi'_{\mathbf{k}} \rangle = gG_{\mathbf{k}}$  and  $\langle \bar{\phi}_{\mathbf{k}} \phi_{\mathbf{k}} \rangle = \langle \bar{\phi}'_{\mathbf{k}} \phi_{\mathbf{k}} \rangle = g(G_{\mathbf{k}} + 1)$  for fields from the same sublattice ( $\bar{\phi} = a, b$ ), and  $\langle a_{\mathbf{k}} b_{\mathbf{k}} \rangle = \langle \bar{a}_{\mathbf{k}} \bar{b}_{\mathbf{k}} \rangle = -gF_{\mathbf{k}}$  for fields from different sublattices. In the latter case the correlators are unchanged by a replacement  $\bar{\phi} \rightarrow \bar{\phi}'$ . We have defined  $G_{\mathbf{k}} = (n_{\mathbf{k}} + 1/2)(1 - \gamma_{\mathbf{k}}^2)^{-1/2} - 1/2$  and

$F_{\mathbf{k}} = (n_{\mathbf{k}} + 1/2)\gamma_{\mathbf{k}}(1 - \gamma_{\mathbf{k}}^2)^{-1/2}$  where  $n_{\mathbf{k}} = (e^{\beta E_{\mathbf{k}}} - 1)^{-1}$  is the bosonic occupation number. For strong frustration ( $\alpha > 1/2$ ) the stiffness becomes negative and the spin-wave velocity is ill defined due to the presence of unstable modes in the center of the BZ (see Fig. 1).

Starting from this action with bilinear and quartic terms, we implement a renormalization procedure as follows. In successive steps, the modes of highest energy (an infinitesimal fraction of all modes) are integrated out. This decimation of modes yields an effective theory for the remaining modes and gives rise to differential flow equations. As flow parameter we choose  $l = \frac{1}{2} \ln(A_{\text{BZ}}/A_{\text{RBZ}})$ , where  $A_{\text{BZ}} = 2\pi^2$  is the area of the original BZ, and  $A_{\text{RBZ}}$  is the area of the residual BZ (RBZ) populated by the remaining modes. On large length scales in the Néel phase, the RBZ becomes circular and  $l$  is the usual logarithmic length scale. The evolution of the RBZ and the single-magnon dispersion is illustrated in Fig. 1 for various parameters.

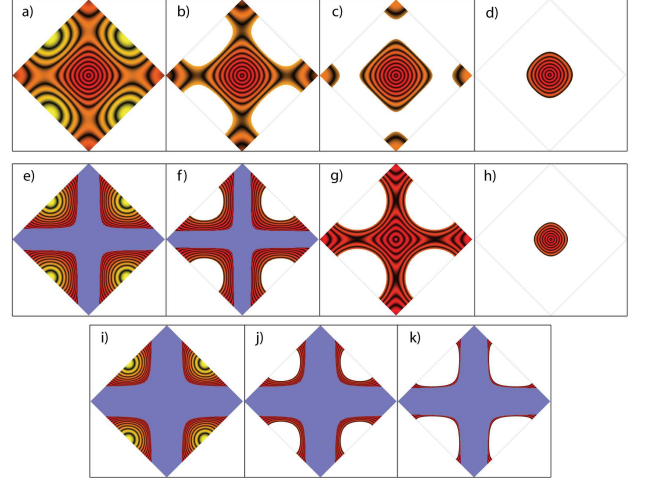


FIG. 1: Evolution of modes under coarse graining. Each panel corresponds to the area  $|k_x| \leq \pi, |k_y| \leq \pi$ . Red color represents small, yellow high positive energy. Black lines are lines of constant energy, blue areas represent unstable modes. Panels (a)-(d): In the Néel phase the RBZ may become disconnected first, then always shrinks to a sphere (here  $S = 1/2$ ,  $\alpha = 0.3$ ,  $l = 0, 0.25, 0.5, 1.0$ ). Panels (e)-(h): In the Néel phase for strong frustration  $\alpha > 1/2$ , initially unstable modes (blue area) are renormalized to stable modes and the RBZ eventually also shrinks to a sphere (here  $S = 1/2$ ,  $\alpha = 0.55$ ,  $l = 0, 0.11, 0.29, 1.30$ ). Panels (i)-(k): In the columnar phase, after the elimination of all stable modes, an area of unstable modes survives (here  $S = 2$ ,  $\alpha = 0.6$ ,  $l = 0, 0.10, 0.20$ ).

To one-loop order, corresponding to a systematical calculation of corrections in order  $1/S$ , the renormalization effects due to spin-wave interactions can be captured by a flow of the single-magnon parameters. The resulting

flow equations are given by

$$dg^{-1} = -\frac{1}{S}dG^0, \quad (3a)$$

$$dJ_1 = \frac{g}{S}J_1(dF^- - 2dG^0), \quad (3b)$$

$$dJ_2 = \frac{g}{S}J_2(dG^+ - 2dG^0), \quad (3c)$$

where the integrals over the differential fraction  $\partial$  of modes of highest energy are defined as  $dG^0 = \int_{\mathbf{q}}^{\partial} G_{\mathbf{q}}$ ,  $dG^+ = \int_{\mathbf{q}}^{\partial} (J_{\mathbf{q}}^+/J_0^+)G_{\mathbf{q}}$ , and  $dF^- = \int_{\mathbf{q}}^{\partial} (J_{\mathbf{q}}^-/J_0^-)F_{\mathbf{q}}$ .

Since the BZ does not remain self-similar under mode decimation, we omit the usual rescaling of length and time which is necessary only for the identification of fixed points under a renormalization-group flow. However, dropping this rescaling does not lead to a loss of information. Then, a fixed point represents an antiferromagnetically ordered phase. The quantum-disordered phase and the transition into it show up as run-away flow.

Because of the changing geometry of the RBZ and the incorporation of the full single-magnon dispersion in our renormalization approach, the flow equations can be integrated up only numerically. Here, we focus on  $T = 0$ , although the flow equations are valid also for  $T > 0$ . The flow of parameters is characterized by the following tendencies. Both exchange couplings  $J_{1,2}$  as well as  $1/g$  always shrink. These fundamental parameters flow in such a way that  $\alpha$  always decreases,  $c^2$  increases (initially it is negative for  $\alpha > 1/2$ ), while  $\rho$  may increase for small  $l$  until it decreases for sufficiently large  $l$ .

The nature of magnetic order can be identified from the flow behavior. Three possibilities are observed. (i) The RBZ shrinks to a circle of decreasing radius  $\propto e^{-l}$  [see Fig. 1 panels (a)-(d) and panels (e)-(h)] while  $J_{1,2}$  and  $g$  (as well as the derived quantities  $c$ ,  $\rho$ ,  $\alpha$ ) converge to positive values. Then Néel order is present, characterized by these renormalized low-energy parameters. (ii) At some finite  $l^*$ , fluctuations become so strong that  $g$  diverges and  $J_{1,2}$  vanish. This indicates the loss of magnetic order due to overwhelming quantum fluctuations. Close to the transition to the Néel phase, the magnetic correlation length – which can be identified with  $\xi = e^{l^*}$  – diverges algebraically like  $\xi \sim (\alpha - \alpha_c)^{-1}$ . For  $S = 1/2$  this asymptotic behavior is shown in one inset of Fig. 2. (iii) For strong frustration, it is also possible that a finite RBZ of unstable modes remains after decimation of *all* stable modes (see Fig. 1 panels (i)-(k)). This indicates that the instability towards columnar order is effective for the renormalized low-energy modes.

The region of stability of the Néel phase is illustrated by the light grey region in Fig. 2. In the absence of frustration, we find Néel order to be stable for  $1/S \lesssim 5.09$  in remarkable agreement with conventional linear SWT [4]. However, this is pure coincidence since in linear SWT the phase boundary is determined by the vanishing of the local magnetization calculated in order  $S^0$ , whereas

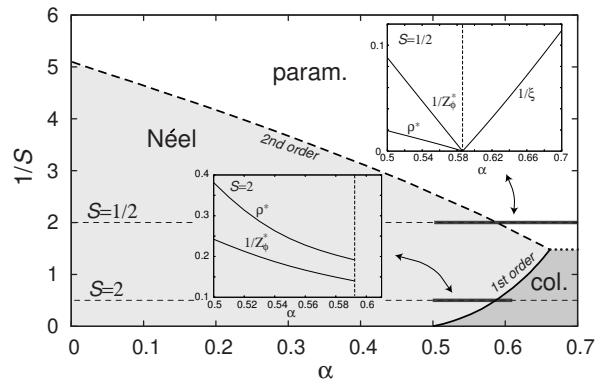


FIG. 2: Phase diagram showing the 2nd order transition line between the Néel ordered and the PM phase (dashed line) and the 1st order boundary between the Néel and the columnar phase (solid line). The border between the PM and the columnar phase (dotted line) is just guesswork and cannot be calculated within our approach. Insets: Nature of the phase transitions. For  $S = 1/2$  the renormalized spin stiffness  $\rho^*$  vanishes and the strength of the quantum fluctuations  $Z_\phi^*$  diverges at the phase boundary corresponding to a 2nd order transition. Close to the the Néel phase the correlation length diverges like  $\xi \sim (\alpha - \alpha_c)^{-1}$ . At the 1st order transition ( $S = 2$ )  $\rho^*$  and  $Z_\phi^*$  remain finite.

here it is determined by the divergence of  $g$  due to spin-wave interactions treated in one-loop order. While the phase boundary is located at academically small spin values for small frustration,  $S$  reaches physically meaningful values at larger frustration where the discrepancies between SWT and our renormalization approach become more pronounced. In linear SWT, the phase boundary smoothly approaches  $1/S \searrow 0$  for  $\alpha \nearrow 0.5$ , whereas we find the Néel phase to reach up to  $\alpha = 0.66$  for  $S = 0.68$ . For spins smaller than this value, the Néel phase becomes unstable towards a PM phase via a second-order transition, whereas it becomes unstable towards columnar order for  $S > 0.68$  via a first order transition.

In the region where the Néel phase reaches up to  $\alpha > 1/2$ , initially unstable modes are renormalized to stable ones by spin-wave interactions. Simultaneously,  $\alpha$  is renormalized to a value  $\alpha^* < 1/2$  and the flow behavior (i) is realized. In the columnar phase, the flow of  $\alpha$  saturates at a value  $\alpha^* > 1/2$  and the flow behavior (iii) is observed.

Stability of Néel order for  $\alpha > 0.5$  so far has been found only by a self-consistently modified SWT [14] and Schwinger-boson mean-field theory (SBMFT) [15]. The overall shape of the Néel phase of these approaches is consistent with our findings. However, in modified SWT and SBMFT the first-order transition from Néel to columnar order can be obtained only by a comparison of free energies between the two phases. In our theory, the transition directly emerges from the analysis of spin-wave interactions in the Néel phase.

The nature of the transitions out of the Néel phase becomes apparent from the behavior of the fluctuations on large length scales ( $k \rightarrow 0$ ), where  $\langle \phi_{\mathbf{k}} \phi'_{\mathbf{k}} \rangle \simeq \frac{Z_\phi}{\sqrt{2k}}$  with  $Z_\phi \equiv \frac{q}{\sqrt{1-2\alpha}} \propto \frac{c}{\rho}$ . Approaching the transition into the PM phase, the renormalized value  $Z_\phi^*$  diverges and gives rise to a divergent susceptibility (see Fig. 3). At the same time the renormalized  $\rho^*$  vanishes while  $c^*$  remains finite. The continuous evolution of  $Z_\phi^*$  and  $\rho^*$  indicate the second-order nature of the transition. Approaching the transition into the columnar phase, one observes a saturation of  $Z_\phi^*$  and  $\rho^*$  at finite values as well as a discontinuous jump of  $\alpha^*$  indicating a first-order transition. Fig. 3 illustrates the dependence of various renormalized quantities on  $\alpha$  and  $1/S$  within the Néel phase. The insets of Fig. 2 show the evolution of  $\rho^*$ ,  $Z_\phi^*$  and  $\xi$  with higher resolution at the transitions.

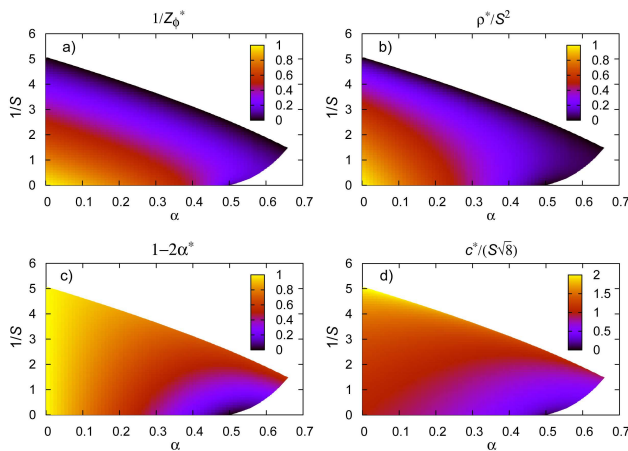


FIG. 3: Values of the renormalized parameters within the Néel phase. Color corresponds to the strength of large-scale fluctuations (a), the renormalized spin stiffness (b), the frustration (c), and the spin-wave velocity (d).

Confidence in the reliability of our findings is provided by quantitative comparisons for specific parameter values. Results for  $Z_c^* \equiv c^*/c$  exist from various approaches. For  $S = 1/2$  and  $\alpha = 0$ , first-order SWT yields a slight enhancement of spin-wave velocity,  $Z_c^{\text{SWT}} = 1.158$ . We find an increased value  $Z_c^* = 1.20$ , which is in agreement with Monte Carlo (MC) simulations (see [16] and references therein). As  $1/S$  and/or  $\alpha$  increases, the enhancement factor  $Z_c^*$  also increases. At the phase boundary  $1/S \approx 5.09$  for  $\alpha = 0$ , the difference is already more pronounced:  $Z_c^{\text{SWT}} = 1.40$  and  $Z_c^* = 2.04$ . For  $\alpha > 0$ , unfortunately, MC data for  $Z_c$  are not available at the transition out of the Néel phase, neither for  $S = 1/2$  nor for larger physical values of  $S$ .

In conclusion, we have presented a novel renormalization approach for frustrated quantum antiferromagnets which fully accounts for the underlying lattice geometry and consistently captures the renormalization of the

single-magnon parameters by spin-wave interactions all over the magnetic BZ. For the  $J_1$ - $J_2$  model our approach yields a unifying description of the second-order transition between the Néel phase and the PM phase and the first-order transition between the Néel phase and the columnar phase.

Our approach still falls short of a proper treatment of topological aspects, which go far beyond a theory of interacting spin waves. However, a comparison of our results to data from experiments and simulations will allow to deduce more explicitly the quantitative significance of the topological terms for the location of the border of the Néel phase as well as its renormalized spin-wave parameters. Although our one-loop theory is not exact (in particular, critical exponents for the transition from the Néel to the PM phase are only approximate [7]), we expect artefacts of the one-loop approximation to be relevant only for the asymptotic large-scale behavior, but less for the values of non-divergent quantities such as  $Z_c^*$  or the location of the phase boundary.

For  $S = 1/2$ , exact diagonalization provides evidence for the breakdown of Néel order near  $\alpha \approx 0.35$  [17] which is notably smaller than our value  $\alpha \approx 0.58$ . This deviation may be considered as quantitative measure for the relevance of topological excitations. It would be desirable to have numerical results for  $S = 2$ , where topological excitations do not play a role and agreement with our theory should be much better.

This work was supported by Deutsche Forschungsgemeinschaft SFB 608.

- 
- [1] S. Sachdev, *Quantum Phase Transitions* (Cambridge University Press, Cambridge, England, 1999).
  - [2] T. Senthil, L. Balents, S. Sachdev, A. Vishwanath, and M. P. A. Fisher, *Phys. Rev. B* **70**, 144407 (2004).
  - [3] O. P. Sushkov, J. Oitmaa, and Z. Weihong, *Phys. Rev. B* **63**, 104420 (2001).
  - [4] P. Chandra and B. Douçot, *Phys. Rev. B* **38**, R9335 (1988).
  - [5] F. D. M. Haldane, *Phys. Rev. Lett.* **61**, 1029 (1988).
  - [6] E. Fradkin and M. Stone, *Phys. Rev. B* **38**, R7215 (1988).
  - [7] S. Chakravarty, B. I. Halperin, and D. R. Nelson, *Phys. Rev. B* **39**, 2344 (1989).
  - [8] N. Read and S. Sachdev, *Phys. Rev. Lett.* **62**, 1694 (1989).
  - [9] N. Read and S. Sachdev, *Phys. Rev. B* **42**, 4568 (1990).
  - [10] P. Hasenfratz, *Eur. Phys. J. B* **13**, 11 (2000).
  - [11] F. Krüger and S. Scheidl, unpublished.
  - [12] J. M. Radcliffe, *J. Phys. A* **4**, 313 (1971).
  - [13] The analogy  $a \rightarrow b$  is given by the correspondences  $\hat{S}_z \rightarrow -\hat{S}_z$  and  $\hat{S}_\pm \equiv \hat{S}_x \pm i\hat{S}_y \rightarrow \hat{S}_\mp$ .
  - [14] J. H. Xu and C. S. Ting, *Phys. Rev. B* **42**, R6861 (1990).
  - [15] F. Mila, D. Poilblanc, and C. Bruder, *Phys. Rev. B* **43**, 7891 (1991).
  - [16] E. Manousakis, *Rev. Mod. Phys.* **63**, 1 (1991).
  - [17] H. J. Schulz, T. A. L. Ziman, and D. Poilblanc, *J.*

Physique I **6**, 675 (1996).